

Segmentation by Level Sets and Symmetry

Tammy Riklin-Raviv Nahum Kiryati Nir Sochen

Tel Aviv University, Tel Aviv 69978, Israel

tammy@eng.tau.ac.il

nk@eng.tau.ac.il

sochen@post.tau.ac.il

Abstract

Shape symmetry is an important cue for image understanding. In the absence of more detailed prior shape information, segmentation can be significantly facilitated by symmetry. However, when symmetry is distorted by perspective, the detection of symmetry becomes non-trivial, thus complicating symmetry-aided segmentation.

We present an original approach for segmentation of symmetrical objects accommodating perspective distortion. The key idea is the use of the replicative form induced by the symmetry for challenging segmentation tasks. This is accomplished by dynamic extraction of the object boundaries, based on the image gradients, gray levels or colors, concurrently with registration of the image symmetrical counterpart (e.g. reflection) to itself. The symmetrical counterpart of the evolving object contour supports the segmentation by resolving possible ambiguities due to noise, clutter, distortion, shadows, occlusions and assimilation with the background. The symmetry constraint is integrated in a comprehensive level-set functional for segmentation that determines the evolution of the delineating contour. The proposed framework is exemplified on various images of skew-symmetrical objects and its superiority over state of the art variational segmentation techniques is demonstrated.

1. Introduction

Shape symmetry is a useful visual feature for image understanding [1, 8, 11, 12, 15, 20, 21, 31, 33, 36, 35]. This research employs symmetry for object detection and segmentation. In the presence of noise, clutter, distortion, shadows, occlusions or assimilation with the background, segmentation becomes challenging. In these cases, object boundaries do not fully correspond to edges in the image and may not delimit homogeneous image regions. Hence, classic region-based and edge based segmentation techniques are not sufficient. We, therefore, suggest a novel approach to facilitate segmentation of symmetrical objects by using their replicative form induced by the symmetry. The model presented is applicable for translational-symmetry, rotational-symmetry

and bilateral symmetry (reflection).

In a level set framework for segmentation [23], images are represented via level-set functions where the object regions are assigned to the positive levels. The resulting parameterization-free shape description eliminates the need to relate shape as a collection of points or features, giving a meaningful interpretation to dissimilarity measure between shapes. Moreover, any transformation applied on the image changes the coordinate system of its level-set function. The represented shape is thus transformed correspondingly, simplifying the process of shape alignment.

The proposed method for symmetry-aided segmentation benefits from the level-set formulation. Regarding shape as one entity, we apply a symmetry operator on its level-set representation to obtain its symmetrical counterpart. We then use the distance between the shape representations to impose a shape constraint that facilitates the segmentation. This approach is, thus, considerably different from other methods that support segmentation by symmetry [9, 16, 18, 34].

When symmetry is distorted by perspective, the detection of symmetry becomes non-trivial, thus complicating symmetry aided segmentation. We approach this difficulty by showing that an image of a symmetrical object, distorted by a projective transformation, relates to its symmetrical counterpart (e.g. reflection) by a projective transformation. The explicit form of the homography between symmetrical counterparts is shown and is used to define the limits on the ability to recover the distorting projective transformation.

The paper contains two fundamental contributions. The first is the use of intrinsic shape property - symmetry - as a prior for image segmentation. The second is a theoretical result concerns with symmetrical objects distorted by projective transformations which has significant implications related also to 3D object reconstruction. We thus present unified framework for segmentation of symmetrical objects distorted by perspective, integrating region-based, edge-based, smoothness and symmetry constraints. The proposed method is exemplified and verified on various images of roughly symmetrical objects in the presence of projective distortion.

2. Level sets for segmentation

In this section we review state of the art segmentation with level sets. We describe and generalize fundamental concepts of the two-phase region based segmentation approach of Vese and Chan [3, 32]. We then recall the basics of geometric active contours as introduced in [2] extended in [14] and represented in [13]. These are incorporated within the Chan-Vese level-set formulation. In the subsequent sections we show how the symmetry cue can be integrated, to establish a unified level set framework that efficiently exploits all image features essential for segmentation.

2.1. Region-based term

Let $I: \Omega \rightarrow \mathbb{R}^+$ denote a gray level image, where $\Omega \subset \mathbb{R}^2$ is the image domain. Let ω be open subset of Ω . In the spirit of the Mumford-Shah model [22], we define a boundary $C \in \Omega$, $C = \partial\omega$ that delimits homogeneous regions in I . Thus, for a general feature $G(I)$, in the particular two phase case, we look for a curve C that maximizes the difference between two scalars u_+ and u_- defined as follows:

$$u_+ = A^+ \int_{\omega} G^+(I(\mathbf{x}))d\mathbf{x} \quad u_- = A^- \int_{\Omega \setminus \omega} G^-(I(\mathbf{x}))d\mathbf{x} \quad (1)$$

where $\mathbf{x} \equiv (x, y)$, $A^+ = 1/\int_{\omega} d\mathbf{x}$ and $A^- = 1/\int_{\Omega \setminus \omega} d\mathbf{x}$. The feature chosen depends on the image homogeneity. In the work of Chan and Vese [3] the image is approximated by a piecewise constant function whose values are given by $G^+(I(x)) = G^-(I(x)) = I(x)$. Hence $u_+ = \overline{I_{in}}$ and $u_- = \overline{I_{out}}$ are the average gray levels in the object regions and in the background regions respectively. In this study we use the average gray level and the variance:

$$G^+(I) = (I(\mathbf{x}) - \overline{I_{in}})^2 \quad G^-(I) = (I(\mathbf{x}) - \overline{I_{out}})^2 \quad (2)$$

This was considered by [32] and by [19] in the past. In [27] a probabilistic formulation to G has been proposed.

In the level set framework for curve evolution [23], an evolving curve $C(t)$ is defined as the zero level of a level set function $\phi: \Omega \rightarrow \mathbb{R}$ at time t :

$$C(t) = \{\mathbf{x} \in \Omega \mid \phi(\mathbf{x}, t) = 0\}. \quad (3)$$

Following [3], the Heaviside function of ϕ

$$H(\phi(t)) = \begin{cases} 1 & \phi(t) \geq 0 \\ 0 & \text{otherwise} \end{cases} \quad (4)$$

is used to indicate the object-background regions in the image that correspond the non-negative and negative levels in

ϕ , respectively. Practically, a smooth approximation of the Heaviside function H_{ϵ} is used [3]:

$$H_{\epsilon}(\phi) = \frac{1}{2} \left(1 + \frac{2}{\pi} \arctan\left(\frac{\phi}{\epsilon}\right) \right) \quad (5)$$

The above formulation enables the construction of a region based cost functional with a well defined integration domain:

$$\begin{aligned} E_{RB}(\phi) = & \int_{\Omega} [(\mathbf{G}^+(I(\mathbf{x})) - \mathbf{u}_+)^2 H_{\epsilon}(\phi) \\ & + (\mathbf{G}^-(I(\mathbf{x})) - \mathbf{u}_-)^2 (1 - H_{\epsilon}(\phi))] d\mathbf{x} \end{aligned} \quad (6)$$

where the subscript RB stands for region-based. We use boldface to denote vectors. The optimal curve would best separate its interior from its exterior with respect to their relative characteristic scalars (or vectors) u_+ and u_- . Note, that the functional minimizer is ϕ . The evolving boundary $C(t)$ is derived from $\phi(t)$ using (3). The level set function ϕ is updated according to:

$$\phi_t^{RB} = \delta_{\epsilon}(\phi) [(\mathbf{G}^-(I(\mathbf{x})) - \mathbf{u}_-)^2 - \mathbf{G}^+(I(\mathbf{x})) - \mathbf{u}_+)^2] \quad (7)$$

The evolution of ϕ at each time steps is weighted by the derivative of the regularized form of the Heaviside function:

$$\delta_{\epsilon}(\phi) = \frac{dH_{\epsilon}(\phi)}{d\phi} = \frac{1}{\pi} \frac{\epsilon}{\epsilon^2 + \phi^2}$$

2.2. Geodesic active contour term

Edge based segmentation approaches usually define the object boundaries by the local maxima of the image gradients. Let $\nabla I(x, y) = (I_x, I_y)^T = \left(\frac{\partial I(x, y)}{\partial x}, \frac{\partial I(x, y)}{\partial y} \right)^T$ denote the vector field of the image gradients. The inverse edge indicator function is defined by;

$$g(\mathbf{x}) = 1/(1 + |\nabla I|^2) \quad (8)$$

Let s be an arc-length parameter. The geodesic active contour functional $\int_0^L g(C(s))ds$ integrates the inverse edge indicator along the curve. A minimizer C will be obtained when $g(C(s))$ vanishes, that is when the contour C is aligned with the image edges. The corresponding term for ϕ takes the form:

$$E_{GAC} = \int_{\Omega} g(|\nabla I|) |\nabla H_{\epsilon}(\phi(\mathbf{x}))| d\mathbf{x}, \quad (9)$$

and the evolution of ϕ is determined by:

$$\phi_t^{GAC} = \delta_{\epsilon}(\phi) \operatorname{div} \left(g(|\nabla I|) \frac{\nabla \phi}{|\nabla \phi|} \right). \quad (10)$$

Thus, the zero level of ϕ is constrained to follow the image gradients. When $g = 1$ Eq. 10 reduces to:

$$E_{LEN} = \int_{\Omega} |\nabla H_{\epsilon}(\phi(\mathbf{x}))| d\mathbf{x} \quad (11)$$

This functional measures the curve length $|C|$ and usually indicates the curve smoothness [3]. Minimizing (11) with respect to ϕ , we obtain the following evolution equation:

$$\phi_t^{LEN} = \delta_{\epsilon}(\phi) \operatorname{div} \left(\frac{\nabla \phi}{|\nabla \phi|} \right). \quad (12)$$

2.3. Alignment term

The geodesic active contour term (9) determines the location of the zero level of ϕ . In [14] it is suggested to incorporate the directional edge information to refine the segmentation. This is done by aligning the level set normal direction, $\vec{n} = \frac{\nabla \phi}{|\nabla \phi|}$ with the image gradients direction ∇I .

$$E_{RA} = - \int_{\Omega} |\langle \nabla I, \frac{\nabla \phi}{|\nabla \phi|} \rangle| |\nabla H_{\epsilon}(\phi)| d\mathbf{x}. \quad (13)$$

where RA refer to *robust alignment*, as defined in [13]. The associated gradient descent equation:

$$\phi_t^{RA} = -\delta_{\epsilon}(\phi) \operatorname{sign}(\langle \nabla \phi, \nabla I \rangle) \Delta I \quad (14)$$

2.4. Shape term

The image data by itself is not sufficient for accurate object extraction in the presence of noise, occlusions or assimilation with the background. Recent variational approaches for segmentation suggest to incorporate a prior shape constraint to facilitate segmentation [4, 5, 6, 7, 17, 24, 28, 30]. When only a single image is given, such prior is not available. Nevertheless, if an object is known to be symmetrical, its replicative form, induced by the symmetry, can be used. Section 4 considers the incorporation of the symmetry constraint within a level-set framework for segmentation. The formulation is established based on a result shown in section 3.

3. Symmetry and Projectivity

3.1. Symmetry

An object is symmetrical with respect to a given operation if it remains invariant under that operation. In 2D geometry these operations relate to the basic Euclidean plane isometries: reflection, inversion, rotation and translation. We denote a symmetry operation by S . S is an isometry operating on homogeneous vectors $\mathbf{x} = (x, y, 1)^T$ represented as

$$S = \begin{vmatrix} \mathbf{s}R & \mathbf{t} \\ \mathbf{0}^T & 1 \end{vmatrix} \quad (15)$$

where \mathbf{t} is a translation 2D vector, $\mathbf{0}$ is a null 2D vector, R is the 2×2 rotation matrix and \mathbf{s} is the diagonal matrix $\operatorname{diag}(\pm 1, \pm 1)$.

Specifically, we relate to either of the following transformations:

1. S is translation if $\mathbf{t} \neq \mathbf{0}$ and $\mathbf{s} = R = \operatorname{diag}(1, 1)$.
2. S is rotation if $\mathbf{t} = \mathbf{0}$ and $\mathbf{s} = \operatorname{diag}(1, 1)$.
3. S is reflection if $\mathbf{t} = \mathbf{0}$, $R = \operatorname{diag}(1, 1)$ and \mathbf{s} is either $\operatorname{diag}(-1, 1)$ for left-right reflection or $\operatorname{diag}(1, -1)$ for up-down reflection.

In the case of reflection, the symmetry operation *reverses orientation*, otherwise (translation, rotation and inversion) it is *orientation preserving*.

Definition 1 Let I denote an image defined w.l.o.g. on the symmetrical domain $\Omega = [-a, a] \times [-b, b]$, I is symmetrical with respect to S , if

$$I(\mathbf{x}) = I(S\mathbf{x}) \text{ for each } \mathbf{x} \in \Omega. \quad (16)$$

$\hat{I}(\mathbf{x}) \equiv I(S\mathbf{x})$ is the symmetrical counterpart of I with respect to S .

An image is identical to its symmetrical counterpart, if and only if it is symmetrical.

We claim that the image of a symmetrical object distorted by a projectivity is related to its symmetrical counterpart by projective transformation different from the defining symmetry. Before we proceed proving this claim we recall the definition of projective transformation.

3.2. Projectivity

This subsection follows the definitions in [10].

Definition 2 A planar projective transformation (*projectivity*) is a linear transformation represented by a non-singular 3×3 matrix \mathcal{H} operating on homogeneous vectors, $\mathbf{x}' = \mathcal{H}\mathbf{x}$, where,

$$\mathcal{H} = \begin{bmatrix} h_{11} & h_{12} & h_{13} \\ h_{21} & h_{22} & h_{23} \\ h_{31} & h_{32} & h_{33} \end{bmatrix} \quad (17)$$

Important specializations of the group formed by projective transformation are the affine group and the similarity group which is a subgroup of the affine group. These groups form a hierarchy of transformations. A similarity transformation is represented by

$$\mathcal{H}_S = \begin{bmatrix} \kappa R & \mathbf{t} \\ \mathbf{0}^T & 1 \end{bmatrix} \quad (18)$$

where R is a 2×2 rotation matrix and κ is an isotropic scaling. When $\kappa = 1$, \mathcal{H}_S is the Euclidean transformation

denoted by \mathcal{H}_E . An affine transformation is obtained by multiplying the matrix \mathcal{H}_S with

$$\mathcal{H}_A = \begin{bmatrix} K & \mathbf{0} \\ \mathbf{0}^T & 1 \end{bmatrix}. \quad (19)$$

K is an upper-triangular matrix normalized as $|K| = 1$. The matrix \mathcal{H}_P defines the ‘‘essence’’ of the projective transformation and takes the form:

$$\mathcal{H}_P = \begin{bmatrix} I & \mathbf{0} \\ \mathbf{v}^T & v \end{bmatrix}. \quad (20)$$

A projective transformation can be decomposed into a chain of transformations of a descending (or ascending) hierarchy order,

$$\mathcal{H} = \mathcal{H}_S \mathcal{H}_A \mathcal{H}_P = \begin{bmatrix} \mathbf{A} & \mathbf{t} \\ \mathbf{v}^T & v \end{bmatrix} \quad (21)$$

where $v \neq 0$ and $A = \kappa RK + \mathbf{t}\mathbf{v}^T$ is a non-singular matrix.

3.3. Relation between symmetrical counterparts

In this subsection we consider the relation between an image of symmetrical object distorted by planar projective transformation \mathcal{H} and its symmetrical counterpart.

Theorem 1 *Let I_S denote a symmetrical image as defined by (16). The image I_A is obtained from the symmetrical image I_S by applying the planar projective transformation \mathcal{H} : $I_A(\mathbf{x}) = I_S(\mathcal{H}\mathbf{x})$. Let $\hat{I}_A(\mathbf{x}) = I_A(S\mathbf{x})$ denotes the symmetric counterpart of I_A with respect to a symmetry operation S . The images I_A and \hat{I}_A are related by planar projective transformation, represented by a 3×3 matrix of the form*

$$M = S^{-1}\mathcal{H}^{-1}S\mathcal{H}. \quad (22)$$

Proof 1 *The symmetrical counterpart \hat{I}_A can be generated from I_A either by the symmetry operation S or by a projective transformation M .*

$$\begin{aligned} I_A(\mathbf{x}) &= I_A(\mathcal{H}^{-1}\mathcal{H}\mathbf{x}) = I_A(\mathcal{H}^{-1}\mathbf{y}) \\ &= I_S(\mathbf{y}) = I_S(S\mathbf{y}) \\ &= I_S(\mathcal{H}\mathcal{H}^{-1}S\mathbf{y}) \\ &= I_A(\mathcal{H}^{-1}S\mathbf{y}) = I_A(\mathcal{H}^{-1}S\mathcal{H}\mathbf{x}) \\ &= I_A(SS^{-1}\mathcal{H}^{-1}S\mathcal{H}\mathbf{x}) \\ &= \hat{I}_A(S^{-1}\mathcal{H}^{-1}S\mathcal{H}\mathbf{x}) = \hat{I}_A(M\mathbf{x}) \end{aligned} \quad (23)$$

The chain of equalities in (23) is equivalent to the following sequence of operations:

1. Apply the inverse of the projective (distorting) transformation, \mathcal{H}^{-1} on I_A to generate a symmetrical image I_S .

2. Apply the symmetry operation S on I_S , under which it remains invariant.
3. Multiply I_S by the projective transformation matrix \mathcal{H} to obtain back the image I_A .
4. Apply again the symmetry operation S on I_A to obtain its symmetrical counterpart \hat{I}_A .

Let $N = M^{-1} = \mathcal{H}^{-1}S^{-1}\mathcal{H}S$. N and thus M are projective transformations since $\mathcal{H}N = S^{-1}\mathcal{H}S$ is a projective transformation according to:

$$S^{-1}\mathcal{H}S = S^{-1} \begin{bmatrix} \mathbf{A} & \mathbf{t} \\ \mathbf{v}^T & v \end{bmatrix} S = \begin{bmatrix} \mathbf{A}' & \mathbf{t}' \\ \mathbf{v}'^T & v' \end{bmatrix} = \mathcal{H}' \quad (24)$$

The claim is exemplified for two particular cases. Consider the image of the symmetrical object and its left-right reflection shown in Fig. (1)a-b. Suppose that the image symmetry has been distorted by an Euclidean transformation of the form:

$$\mathcal{H}_E = \begin{bmatrix} \cos \theta & -\sin \theta & t_x \\ \sin \theta & \cos \theta & t_y \\ 0 & 0 & 1 \end{bmatrix}$$

Note that the Euclidean transformation is an isometry and thus preserves the object symmetry. However, it draws the symmetry axis of the object away from the symmetry axis of the image, rotating it by angle θ and translating it by t_x . Fig. (1)a relates to its symmetrical counterpart by:

$$M = S^{-1}\mathcal{H}_E^{-1}S\mathcal{H}_E = \begin{bmatrix} \cos 2\theta & -\sin 2\theta & 2t_x \cos \theta \\ \sin 2\theta & \cos 2\theta & 2t_x \sin \theta \\ 0 & 0 & 1 \end{bmatrix},$$

where $S = \text{diag}(-1, 1, 1)$. Fig. (1)a can thus be obtained from Fig. (1)b by a translation by $2R(\theta)[t_x, 0]^T$ and a rotation by 2θ . Note that any translation parallel to the symmetry axis (in this case t_y) cannot be recovered from M .

Consider, next the images shown in Fig. (1)c-d. The object is distorted by a projective transformation \mathcal{H}_P :

$$\mathcal{H}_P = \begin{bmatrix} 1 & 0 & 0 \\ 0 & 1 & 0 \\ v_1 & v_2 & 1 \end{bmatrix}$$

The relation between the two images can be described by:

$$M = S^{-1}\mathcal{H}_P^{-1}S\mathcal{H}_P = \begin{bmatrix} 1 & 0 & 0 \\ 0 & 1 & 0 \\ 2v_1 & 0 & 1 \end{bmatrix}$$

When $v_2 \neq 0$ the object shape is distorted but its symmetry is preserved, thus v_2 cannot be recovered from M . In general, any operation that does not distort the object symmetry can not be recovered from M . Refer to [26] for the complete proof.

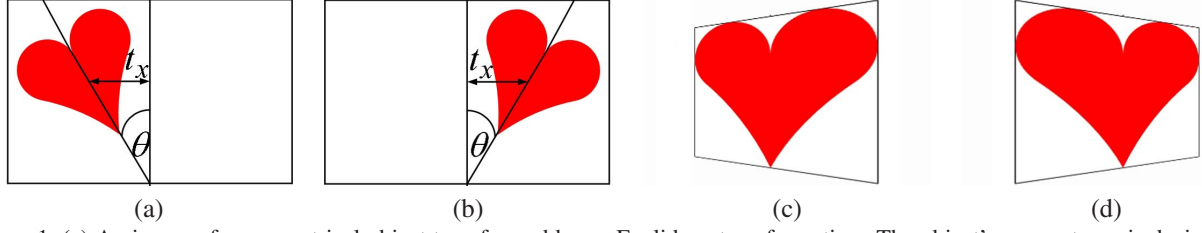


Figure 1. (a) An image of a symmetrical object transformed by an Euclidean transformation. The object’s symmetry axis deviates by t_x and by angle θ from the symmetry axis of the image. (b) The symmetrical counterpart of the image in (a). (c) An image of a symmetrical object distorted by projective transformation. (d) The symmetrical counterpart of the image in (c).

4. Symmetry based segmentation

4.1. Symmetry constraint

The discussion in the previous section related to images. We will now refer to the dynamic object indicator functions represented by $H_\epsilon(\phi(t))$. Let $\hat{\phi}: \Omega \rightarrow \mathbb{R}$ denote the symmetrical counterpart of ϕ with respect to a symmetry operation S . Specifically, $\hat{\phi}(\mathbf{x}) = \phi(S\mathbf{x})$ where S is either a reflection or rotation or translation. We assume that the S is known. We denote by \mathcal{T}_p the alignment function between $H_\epsilon(\phi)$ and $H_\epsilon(\hat{\phi}_S)$. \mathcal{T}_p captures the deviation of the object symmetry axis from that of the image and the projective transformation that distorts its symmetry. Note, however, that this information is not known in advance. \mathcal{T}_p is recovered by a registration process held concurrently with the segmentation, detailed in subsection 4.3.

Let $\mathcal{D} = D(H_\epsilon(\phi), \mathcal{T}_p H_\epsilon(\hat{\phi}))$ denote a dissimilarity measure between the evolving shape representation and its symmetrical counterpart. Note that if \mathcal{T}_p is correctly recovered and ϕ captures a perfectly symmetrical object (up to projectivity) then $\mathcal{D} = 0$. \mathcal{D} thus quantifies the distortions of object symmetry which are not caused by the projectivity. Whenever these distortions are due to false detection of the object boundaries (caused by noise, occlusions, clutter, etc.) and not features of the object shape, \mathcal{D} defines an appropriate symmetry constraint. In [24], \mathcal{D} measures the non-overlapping object-background regions between the evolving segmentation and a well-defined prior $\hat{\phi}$:

$$D(\phi, \hat{\phi}) = \int_{\Omega} \left[H_\epsilon(\phi(\mathbf{x})) - \mathcal{T}_p H_\epsilon(\hat{\phi}(\mathbf{x})) \right]^2 d\mathbf{x}. \quad (25)$$

Nevertheless, since in our case $H_\epsilon(\hat{\phi})$ is identical to $H_\epsilon(\phi)$ up to an isometry, it is subject to the same distortions and thus cannot replace a well defined prior. A different formulation is then needed, to be described in the following subsection.

4.2. Biased shape dissimilarity measure

Consider, for example, the approximately bilateral symmetrical (up to projectivity) images shown in Fig. 2a,d. The

objects symmetry is distorted by either deficiencies or excess parts. We would like to use the symmetry to overcome these shape distortions. Nevertheless, incorporating the unbiased shape constraint (according to Eq. 25) in the cost functional for segmentation, results in the undesired segmentation shown in Fig. 2b,e. The symmetrical counterpart of a level-set function ϕ is as imperfect as ϕ . To support a correct evolution of ϕ by $\hat{\phi}$, we have to account for the specific type of corruption.

Refer again to the dissimilarity measure in Eq. (25). The cost functional integrates the non-overlapping object-background regions in both images indicated by $H_\epsilon(\phi)$ and $H_\epsilon(\hat{\phi})$. This is equivalent to a pointwise exclusive-or (xor) operation integrated over the image domain. We may thus rewrite the functional as follows:

$$D(\phi, \hat{\phi}) = \int_{\Omega} \left[H_\epsilon(\phi) \left(1 - H_\epsilon(\hat{\phi}_T) \right) + \left(1 - H_\epsilon(\phi) \right) \mathcal{T}_p H_\epsilon(\hat{\phi}) \right] d\mathbf{x} \quad (26)$$

Note that the expressions (25) and (26) are approximately identical, since $H_\epsilon(\phi) \approx (H_\epsilon(\phi))^2$ (equality is obtained for $\epsilon \rightarrow 0$). There are two types of ‘disagreement’ between the labeling of $H_\epsilon(\phi)$ and $\mathcal{T}_p H_\epsilon(\hat{\phi})$. The first additive term in the right hand side of (26) does not vanish, if there exist image regions labeled as *object* by ϕ and labeled as *background* by its symmetrical counterpart $\hat{\phi}$. The second additive term of (26) does not vanish if there exist image regions labeled as *background* by ϕ and labeled as *object* by $\hat{\phi}$. We can change the relative contribution of each term by a relative weight parameter $\mu \geq 0$:

$$E_S(\phi, \hat{\phi}) = \int_{\Omega} \left[\mu H_\epsilon(\phi) \left(1 - \mathcal{T}_p H_\epsilon(\hat{\phi}) \right) + \left(1 - H_\epsilon(\phi) \right) \mathcal{T}_p H_\epsilon(\hat{\phi}) \right] d\mathbf{x} \quad (27)$$

The associated gradient equation for ϕ is then:

$$\phi_t^S = \delta_\epsilon(\phi) [\mathcal{T}_p H_\epsilon(\hat{\phi}) - \mu(1 - \mathcal{T}_p H_\epsilon(\hat{\phi}))] \quad (28)$$

Now, if excess parts are assumed, the left penalty term should be dominant, setting $\mu > 1$. Otherwise, if deficiencies are assumed, the right penalty term should be domi-

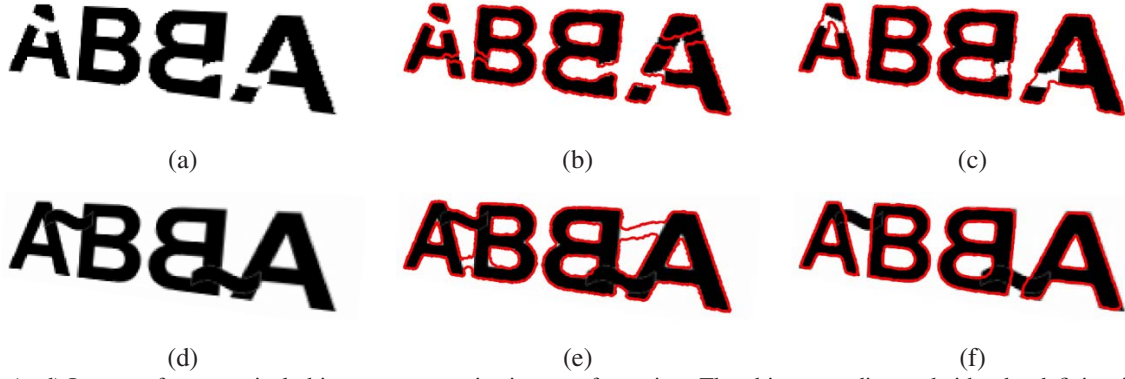


Figure 2. (a, d) Images of symmetrical objects up to a projective transformation. The objects are distorted either by deficiencies (a) or by excess parts (d). (b, e) Segmentation (red) of the images in (a) and (d) respectively, using *unbiased* dissimilarity measure between ϕ and its transformed reflection as in Eq. (25). Object segmentation is further spoiled due to the imperfection in its reflection. (c, f) Successful segmentation (red) using the *biased* dissimilarity measure as in Eq. (27).

nant, setting $\mu < 1$. Fig. 2c,f show segmentation of symmetrical objects with either deficiencies or excess parts, incorporating the shape term (27) within the segmentation functional. We used $\mu = 0.5$ and $\mu = 2$ for the segmentation of Fig. 2c and Fig. 2f, respectively.

4.3. Recovery of the transformation

We now look for the optimal alignment function \mathcal{T}_p that minimizes E_S defined in eq. (27). The operation of \mathcal{T}_p on $H_\epsilon(\hat{\phi})$ is equivalent to the transformation of the coordinate system of $\hat{\phi}(\mathbf{x})$ by a projective transformation \mathcal{H} .

$$\mathcal{T}_p H_\epsilon(\hat{\phi}(\mathbf{x})) = H_\epsilon(\hat{\phi}(\mathcal{H}\mathbf{x})) \quad (29)$$

The matrix \mathcal{H} is defined in Eq (17). The eight unknown ratios of its entries $\hat{h}_{ij} = h_{ij}/h_{33}$ are recovered through the segmentation process, alternately with the evolution of the level set function ϕ . The parameters \hat{h}_{ij} are obtained by minimizing (27) with respect to each.

$$\frac{\partial \hat{h}_{ij}}{\partial t} = \int_{\Omega} \delta_\epsilon(\mathcal{T}_p(\hat{\phi})) [(1 - H_\epsilon(\phi)) - \mu H_\epsilon(\phi)] \frac{\partial \mathcal{T}_p(\hat{\phi})}{\partial \hat{h}_{ij}} dx \quad (30)$$

Derivation of $\frac{\partial \mathcal{T}_p(\hat{\phi})}{\partial \hat{h}_{ij}}$ is done similarly to [25].

4.4. Unified segmentation functional

Symmetry-based, edge-based, region-based and smoothness constraints can be integrated to establish a comprehensive cost functional for segmentation:

$$E(\phi) = E_{PS} + E_{LEN} + E_{GAC} + E_{RA} + E_S \quad (31)$$

with the equations (6, 11, 9, 13, 27). The evolution of ϕ in each time step, $\phi(t+1) = \phi(t) + \phi_t$ is determined by

$$\phi_t(\phi) = \phi_t^{RB} + \phi_t^{LEN} + \phi_t^{GAC} + \phi_t^{RA} + \phi_t^S \quad (32)$$

using a weighted sum (w_i) of equations (7, 12, 10, 14, 28).

Refinement of the segmentation can be obtained for images with multiple channels, $I: \Omega \rightarrow \mathbb{R}^n$, e.g. color images. The region-based term ϕ_t^{RB} and the alignment term ϕ_t^{RA} sum of the contributions of each channel I_i . Figure 5 demonstrates segmentation of a color image. Further exploration could address the use of Beltrami flow [29].

4.5. Algorithm

The algorithm for segmentation of a symmetrical objects in the presence of projectivities is summarized as follows:

1. Choose an initial level-set function $\phi(t=0)$ that determines the initial contour within the image.
2. Set initial values for the transformation parameters \hat{h}_{ij} . For example set $\mathcal{H} = I$ where I is the identity matrix.
3. Compute u_+ and u_- according to (1), based on the current contour interior and exterior, defined by $\phi(t)$.
4. Generate $\hat{\phi}$, the symmetrical counterpart of ϕ .
5. Update the alignment term \mathcal{T}_p by recovering the transformation parameters h_{ij} . according to (30)
6. Update ϕ using the gradient descent equation (32).
7. Repeat steps 3-6 until convergence.

5. Experiments

We exemplify the proposed algorithm for the segmentation of skew-symmetrical objects. The images are displayed with the initial and final segmenting contours. Segmentation results are compared to those obtained using the functional in Eq. (31) without the symmetry term. The contribution of each term in the gradient descent equation (32)

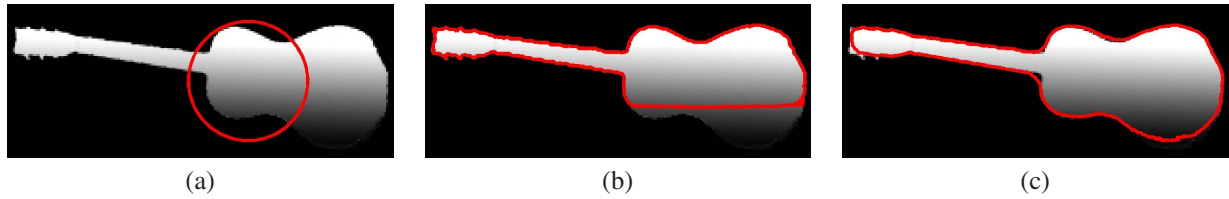


Figure 3. (a) Input image of a roughly symmetrical object with the initial segmentation contour (red). (b) Segmentation (red) without the symmetry constraint. (c) Successful segmentation (red) with the proposed algorithm.



Figure 4. (a) Input image of a roughly symmetrical object with the initial segmentation contour (red). (b) Segmentation (red) without the symmetry constraint. (c) Successful segmentation (red) with the proposed algorithm. Original image courtesy of George Payne. URL: <http://cajunimages.com>

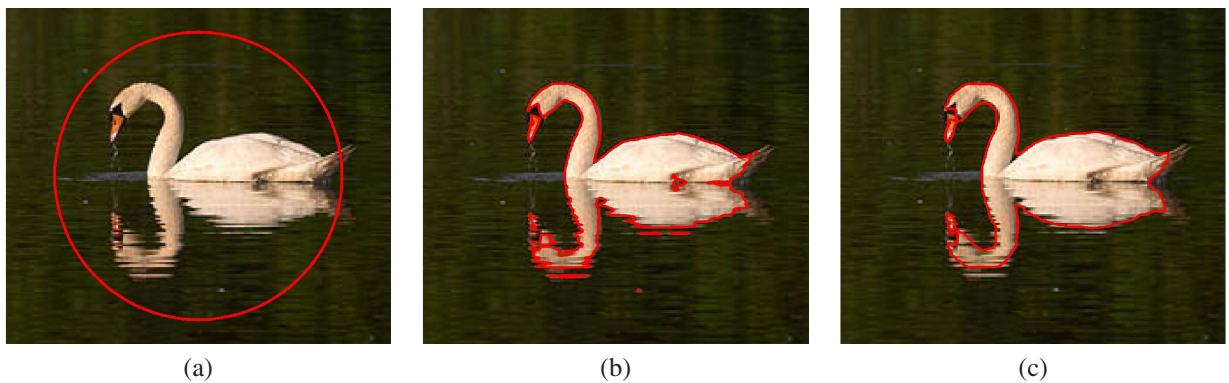


Figure 5. (a) Input image of a roughly symmetrical object with the initial segmentation contour (red). (b) Segmentation (red) without the symmetry constraint. (c) Successful segmentation (red) with the proposed algorithm. Original image courtesy of Richard Lindley. URL: <http://www.richardlindley.co.uk/links.htm>

is normalized to $[-1, 1]$ avoiding the need to “guess” their relative weights. In Fig. 3 the upper part of the guitar is used to extract its lower part correctly. In the butterfly image, Fig. 4, a left-right reflection of the evolving level set function is used to support accurate segmentation of its left wing. In Fig. 5 we used the image colors in addition to the symmetry constraint to facilitate the extraction of the swan and its reflection.

6. Summary

This paper has two major contributions. First, it presents a level-set framework for the segmentation of symmetri-

cal objects distorted by projective transformations. Second, it shows the explicit form of the homography that relates the image of a skew-symmetrical object to its symmetrical counterpart. This homography captures the projective distortion in the object symmetry. It is recovered through the segmentation process, thus revealing an important geometric information on the object of interest.

Acknowledgment

This research was supported by MUSCLE: Multimedia Understanding through Semantics, Computation and Learning, a European Network of Excellence funded by the EC 6th Framework IST Programme.

References

- [1] A. Bruckstein and D. Shaked. Skew-symmetry detection via invariant signatures. *Pattern Recognition*, 31(2):181–192, 1998.
- [2] V. Caselles, R. Kimmel, and G. Sapiro. Geodesic active contours. *IJCV*, 22(1):61–79, Feb. 1997.
- [3] T. Chan and L. Vese. Active contours without edges. *IEEE Transactions on Image Processing*, 10(2):266–277, Feb. 2001.
- [4] Y. Chen, H. Tagare, S. Thiruvankadam, F. Huang, D. Wilson, K. Gopinath, R. Briggs, and E. Geiser. Using prior shapes in geometric active contours in a variational framework. *IJCV*, 50(3):315–328, Dec. 2002.
- [5] D. Cremers, T. Kohlberger, and C. Schnorr. Shape statistics in kernel space for variational image segmentation. *Pattern Recognition*, 36(9):1929–1943, 2003.
- [6] D. Cremers and S. Soatto. A pseudo-distance for shape priors in level set segmentation. In *VLSM*, pages 169–176, 2003.
- [7] D. Cremers, N. Sochen, and C. Schnorr. Multiphase dynamic labeling for variational recognition-driven image segmentation. *IJCV*, 66(1):67–81, 2006.
- [8] L. Davis. Understanding shape, ii: Symmetry. *Trans. on Systems, Man and Cybernetics*, 7:204–212, 1977.
- [9] A. Gupta, V. Prasad, and L. Davis. Extracting regions of symmetry. In *Proceedings of the International Conference on Image Processing*, pages III: 133–136, 2005.
- [10] R. I. Hartley and A. Zisserman. *Multiple View Geometry in Computer Vision*. Cambridge University Press, 2nd edition, 2003.
- [11] W. Hong, Y. Yang, and Y. Ma. On symmetry and multiple view geometry: Structure, pose and calibration from single image. *IJCV*, 60:241–265, 2004.
- [12] K. Kanatani. Symmetry as a continuous feature: Comment. *PAMI*, 19(3):246–247, 1997.
- [13] R. Kimmel. Fast edge integration. In S. Osher and N. Paragios, editors, *Geometric Level Set Methods in Imaging Vision and Graphics*. Springer-Verlag, 2003.
- [14] R. Kimmel and A. Bruckstein. Regularized laplacian zero crossings as optimal edge integrators. *IJCV*, 53(3):225–243, 2003.
- [15] N. Kiryati and Y. Gofman. Detecting symmetry in grey level images: The global optimization approach. *IJCV*, 29(1):29–45, 1998.
- [16] A. Laird and J. Miller. Hierarchical symmetry segmentation. In *Proc. SPIE, Intelligent Robots and Computer Vision IX: Algorithms and Techniques*, volume 1381, pages 536–544, 1991.
- [17] M. Leventon, W. Grimson, and O. Faugeras. Statistical shape influence in geodesic active contours. In *CVPR*, volume I, pages 316–323, 2000.
- [18] T. Liu, D. Geiger, and A. Yuille. Segmenting by seeking the symmetry axis. In *Proceedings of the International Conference on Pattern Recognition*, pages 994–998, 1998.
- [19] L. Lorigo, O. Faugeras, G. W.E.L., R. Keriven, R. Kikinis, A. Nabavi, and C. Westin. Codimension two-geodesic active contours for the segmentation of tabular structures. In *CVPR*, pages 444–451, 2000.
- [20] G. Marola. On the detection of the axes of symmetry of symmetric and almost symmetric planar images. *PAMI*, 11(1):104–108, 1989.
- [21] D. Mukherjee, A. Zisserman, and J. Brady. Shape from symmetry—detecting and exploiting symmetry in affine images. *Phil. Trans. of the Royal Society of London*, 351:77–106, 1995. Series A.
- [22] D. Mumford and J. Shah. Optimal approximations by piecewise smooth functions and associated variational problems. *Communications on Pure and Applied Mathematics*, 42:577–684, 1989.
- [23] S. Osher and J. Sethian. Fronts propagating with curvature-dependent speed: Algorithms based on Hamilton-Jacobi formulations. *J. of Comp. Physics*, 79:12–49, 1988.
- [24] T. Riklin-Raviv, N. Kiryati, and N. Sochen. Unlevel-sets: Geometry and prior-based segmentation. In *ECCV*, volume 4, pages 50–61, 2004.
- [25] T. Riklin-Raviv, N. Kiryati, and N. Sochen. Prior-based segmentation by projective registration and level sets. In *ICCV*, volume I, pages 204–211, 2005.
- [26] T. Riklin-Raviv, N. Kiryati, and N. Sochen. Shape symmetry for segmentation: a level-set approach. Technical report, Tel-Aviv University, 2006.
- [27] M. Rousson and R. Deriche. Adaptive segmentation of vector valued images. In S. Osher and N. Paragios, editors, *Geometric Level Set Methods in Imaging Vision and Graphics*. Springer-Verlag, 2003.
- [28] M. Rousson and N. Paragios. Shape priors for level set representation. In *ECCV*, pages 78–92, 2002.
- [29] N. Sochen, R. Kimmel, and R. Malladi. A general framework for low level vision. *IEEE Transactions on Image Processing*, 7:310–318, 1998. Special Issue on Geometric Active Diffusion.
- [30] A. Tsai, A. Yezzi, Jr., W. Wells, III, C. Tempany, D. Tucker, A. Fan, W. Grimson, and A. Willsky. A shape-based approach to the segmentation of medical imagery using level sets. *Trans. on Medical Imaging*, 22(2):137–154, 2003.
- [31] L. Van Gool, T. Moons, D. Ungureanu, and A. Oosterlinck. The characterization and detection of skewed symmetry. *CVIU*, 61(1):138–150, 1995.
- [32] L. Vese and T. Chan. A multiphase level set framework for image segmentation using mumford and shah model. *IJCV*, 50(3):271–293, 2002.
- [33] Y. Yang, K. Huang, S. Rao, W. Hong, and Y. Ma. Symmetry-based 3-d reconstruction from perspective images. *CVIU*, 99:210–240, 2005.
- [34] Y. Yang, S. Rao, K. Huang, W. Hong, and Y. Ma. Geometric segmentation of perspective images based on symmetry groups. In *ICCV*, volume 2, pages 1251–1258, 2003.
- [35] H. Zabrodsky, S. Peleg, and D. Avnir. Symmetry as a continuous feature. *PAMI*, 17(12):1154–1166, 1995.
- [36] H. Zabrodsky and D. Weinshall. Using bilateral symmetry to improve 3d reconstruction from image sequences. *CVIU*, 67:48–57, 1997.